International Journal of Pharmaceutics 421 (2011) 189–201

Contents lists available at SciVerse ScienceDirect

International Journal of Pharmaceutics

journal homepage: www.elsevier.com/locate/ijpharm

Pharmaceutical Nanotechnology

Cationic ligand appended nanoconstructs: A prospective strategy for brain targeting

Abhinav Agarwal[a], Himanshu Agrawal[b], Shailja Tiwari[c], Sanyog Jain[d], Govind P. Agrawal[a,*]

[a] Pharmaceutics Research Lab, Department of Pharmaceutical Sciences, Dr. H.S Gour University, Sagar 470003, M.P., India
[b] Pharmaceutics Research Laboratory, M.S. University of Baroda, Vadodara 390002, Gujarat, India
[c] Drug Delivery Research Lab, Department of Pharmaceutical Sciences, Dr. H.S Gour University, Sagar 470003, M.P., India
[d] Centre for Pharmaceutical Nanotechnology, Department of Pharmaceutics, National Institute of Pharmaceutical Education and Research, SAS Nagar, Mohali 160062, Punjab, India

ARTICLE INFO

Article history:
Received 16 June 2011
Received in revised form 9 September 2011
Accepted 27 September 2011
Available online 1 October 2011

Keywords:
Blood brain barrier
Doxorubicin
Cationic bovine serum albumin
Solid lipid nanoparticles
Transcytosis

ABSTRACT

The objective of present research was to evaluate the potential of engineered solid lipid nanoparticles (SLNs) as vectors to bypass the blood brain barrier. Anti-cancer agent, doxorubicin (DOX) loaded SLNs were prepared and conjugated with cationic bovine serum albumin (CBSA). The formation of CBSA tethered and plain SLNs were characterized by FTIR, NMR, and TEM analyses. Physicochemical parameters such as particle size/polydispersity index and zeta-potential were also determined. Cellular uptake studies on HNGC-1 cell lines depicted almost six times enhanced uptake of ligand conjugated SLNs as compared to plain DOX solution. Furthermore, CBSA conjugated formulation was more cytotoxic as compared to free drug or unconjugated SLNs. Transendothelial studies showed maximum transcytosis ability of CBSA conjugated SLNs across brain capillary endothelial cells. *In vivo* pharmacokinetic parameters and biodistribution pattern demonstrated efficiency of the system for spatial and temporal delivery of DOX to brain tissues. Lastly, hematological, nephrotoxic as well as hepatotoxic data suggested CBSA conjugated formulations to be less immunogenic compared to plain formulations.

1. Introduction

In the current scenario alleviation of cerebral diseases is still the foremost challenging assignment. This is manifested by inadequacy in delivering therapeutic bioactives across the blood brain barrier (BBB) (Agarwal et al., 2009a). BBB embodies a specialized network of capillary endothelial cells and vascular cellular structures that controls and limits the transport of bioactives into the brain through both physical (tight junctions) and metabolic (enzymes) barriers (Juillerat-Jeanneret, 2008; Begley et al., 2003; Persidsky et al., 2006). The treatment of brain cancers necessitates bypassing the BBB. This is furthermore arduous task since the presence of efflux pump at the BBB actively forces the pharmacological agents out of the CNS (Pardridge, 2003; Begley and Brightman, 2003; Schinkel, 1999). Stress must therefore be focused on developing strategies that augments CNS bioavailability.

In this sequel transport of anticancer bioactives upon encapsulation in different drug delivery systems has been extensively investigated. Amidst of these vehicles vis a vis liposomes (Vyas and Khar, 2002), micelles (Moghimi et al., 2005), nanoparticles [polymeric and solid lipid (SLNs)] (Petri et al., 2007), microspheres (Storm et al., 2002); SLNs have materialized as most rationalized carriers. The use of nontoxic, bioacceptable, biodegradable lipids and possibility of large-scale production are salient facets for parenteral administration (Muller et al., 1997; Schwarz and Mehnert, 1999). Moreover, the ability to form submicron particles, possible sterilization and circumvent toxicity problems are also the potential benefits offered by SLNs (Cavalli et al., 1997; Reddy et al., 2004). Physical stability (several years) and minimized chemical degradation of entrapped drug are very crucial issues that scores SLNs better than liposomes, micelles, emulsions and polymeric nanoparticles (Magenheim et al., 1993; Utreja and Jain, 2001). These vehicles serve as circulating reservoir of cytotoxic agents and thus prevent direct access of drug molecules to healthy tissues/cells. However in absence of a marker (target) nonselective delivery is still visualized. Thus targeting strategy capable of crossing anatomical barriers and in the present case BBB may be instrumental. One such targetor is cationic bovine serum albumin (CBSA) that has been explored to bypass BBB and at the same time does not inherently affect the integrity of BBB tight junction (Thole et al., 2002; Bickel et al., 2001; Xie et al., 2006). The ligand bypasses the BBB via adsorptive transcytosis mechanism involving electrostatic interaction between the positively charged protein and negatively charged membrane cells at the BBB

* Corresponding author at: School of Engg. & Tech., Pharmaceutics Research Laboratory, Department of Pharmaceutical Sciences, Dr. H.S. Gour University, Sagar, M.P., India. Tel.: +91 7582236457; fax: +91 7582236457.
E-mail address: gpagrawal2005@rediffmail.com (G.P. Agrawal).

0378-5173/$ – see front matter © 2011 Elsevier B.V. All rights reserved.
doi:10.1016/j.ijpharm.2011.09.039

(Lu et al., 2005). Previous BBB transcytosis and brain distribution studies demonstrated CBSA to preferentially promote transport of nanoparticles across brain capillary endothelial cells (Lu et al., 2006; Agarwal et al., 2008; Torchilin, 2005).

In the context of drug delivery anthracyclins are the most widely used drugs for brain tumor therapy and doxorubicin (DOX) is the leading drug of this class (Wu and Pardridge, 1999; Brigger et al., 2004). However, use of DOX accompanies possibility of cardiac dysfunctioning including congestive heart failure, arrhythmias, dilated cardiomyopathy and subsequent death. Also a number of other drug related toxicities incorporate alopecia, neutropenia and reactivation of hepatitis B (Agarwal et al., 2009a,b; Martindale, 1996).

Thus in the present study we developed ligand appended SLNs and investigated them as vectors for improving CNS bioavailability. CBSA conjugated SLNs encapsulating DOX were prepared and characterized in terms of morphology, size, and zeta potential. The formulations were then analyzed for *in vitro* release profile. The *in vitro* cellular uptake, cytotoxicity, *in vivo* pharmacokinetics and tissue distribution of SLNs was investigated and compared with free DOX. Further evaluation of cardiotoxicity, hematological parameters and nephrotoxic as well as hepatotoxic effect was studied in Balb/c mice.

2. Materials and methods

2.1. Materials

Doxorubicin was a generous gift from Sun Pharma, Vadodara, Gujarat. Tristearin and soya-lecithin (PC) were benevolent gift samples from Lipiod Pharmaceuticals (Germany). Bovine serum albumin (BSA), 1-ethyl-3-(3-dimethylaminopropyl) carbodiimide (EDAC), stearic acid and cellulose dialysis tubing (MWCO 1000 Da) were procured from Sigma Aldrich (Germany). Nylon membrane filter (0.22 μm) was purchased from Pall Gelman Sciences (USA). Ethylene diamine and cellulose dialysis bag (MWCO 12–14 kDa) were procured from Himedia, India. All other chemicals were of analytical reagent grade and used without any further modification.

2.2. Preparation of solid lipid nanoparticles (SLN-DOX)

SLNs were prepared by melt emulsification and a homogenization technique in accordance with the procedure reported by Jain et al. (2010), Schubert and Muller-Goymann (2003) with minor modifications. Briefly, tristearin (1%, w/v), soya-lecithin (PC; 0.5%, w/v) and stearic acid (0.06%, w/v) were dissolved in a mixture of chloroform and ethanol (1:1, v/v; 10 mL) and the temperature was maintained at 70 °C. Simultaneously, Doxorubicin (DOX; 0.2%, w/v) was dissolved in 10 mL double distilled water containing surfactant Poloxamer 188 (2%, w/v). The lipid melt was injected through a syringe into the stirred aqueous phase, preheated to 5 °C above the temperature of the lipid phase. The dispersion was mechanically (Remi, Mumbai, India) stirred at 3000 rpm for 1 h followed by sonication for 20 min. It was then filtered through membrane filter (0.22 μm) to remove any excess lipid and lyophilized. FTIR spectroscopic studies were carried out by KBr pellet method after adsorption of small quantity of SLNs on KBr pellet using an IR spectroscope (Perkin–Elmer, USA). NMR spectroscopy of the SLNs was carried out at 300 MHz, after dissolving in D_2O (Bruker DRX, USA).

2.3. Preparation of cationic bovine serum albumin (CBSA)

CBSA was prepared from BSA according to the method reported elsewhere with slight modifications (Feng et al., 2009). To recapitulate, 500 mg of bovine serum albumin (BSA) was flooded with slight excess of ethylenediamine (EDA) previously dispersed in conjugation buffer (MES; 0.2 mol/L) at 4 °C while being magnetically stirred (Remi, India) and the pH was maintained to 4.7. Further, 1-ethyl-3-(3-dimethylaminopropyl) carbodiimide (EDAC; 50 mg) was added and incubated for 2 h in dark, at room temperature with stirring. The reaction was terminated by addition of 400 μL of acetate buffer (2 mol/L; pH 4.75). Finally, the solution was dialyzed against distilled water for 48 h and lyophilized.

FTIR spectroscopy of BSA and CBSA was performed in a Perkin–Elmer IR spectroscope following the similar procedure as stated for SLNs. Subsequently, BSA and CBSA were characterized by SDS-PAGE and isoelectric focusing (IEF).

2.4. Preparation of CBSA conjugated DOX loaded SLNs (CBSA-SLN-DOX)

SLN-DOX nanoparticles were suspended in distilled water at a concentration of 20 mg/mL. Fifty milligram N-hydroxy succinimide (NHS) was added and stirred for 6 h followed by addition of 15 mg EDAC and magnetically (Remi, India) stirred for 48 h at room temperature. Subsequently, CBSA (50 mM) was added with overnight stirring (2000 rpm) to facilitate conjugation with the SLNs. The suspension was then eluted through a sepharose column to remove unconjugated CBSA and other impurities and finally lyophilized. FTIR and NMR spectroscopy was carried out following the procedure reported for unconjugated SLNs.

The amount of CBSA coupled to nanoparticles was estimated by measuring the difference between amount of the CBSA added initially in coupling reaction and CBSA recovered in the supernatant after centrifugation of the particulate dispersion at 22,000 rpm for 30 min. Aliquots of the clear supernatants obtained after centrifugation during removal of free CBSA were taken and estimated using bicinchonic acid (BCA) based protein assay (Wiechelman et al., 1988). The quantity of CBSA bound to the nanoparticles was calculated as difference between the initially added CBSA and CBSA, which was recovered after centrifugation.

2.5. Drug content

Lyophilized SLN-DOX (50 mg) were dispersed in double distilled water and extensively dialyzed (MWCO 1000 Da, Sigma, Germany) with magnetic stirring (50 rpm; Remi, Mumbai, India) against double distilled water (DDW) under sink conditions for 10 min to remove any unentrapped drug. Two mg/mL protamine sulfate solution (0.5 mL) was added to facilitate aggregation of SLNs. The dispersion was centrifuged at 25,000 × *g* for 30 min to obtain a pellet. The supernatant was decanted, pellet was washed and freeze dried. The pellet was dissolved in a mixture of methanol–chloroform (1:1, v/v), vortexed and finally centrifuged at 2000 rpm for 15 min. The supernatant was passed through a 0.22-μm membrane filter and loaded on HPLC system. Similar procedure was followed to estimate the drug entrapped in CBSA-SLN-DOX.

Estimation of DOX was carried in accordance with the procedure stated by Reddy et al., with slight modifications using HPLC (Shimadzu, C18, Japan) and at ambient temperature. The flow rate was maintained at 1.5 mL/min at pressure of 102/101 bar, the run time of DOX was found to be 21 min. Peaks of the eluent were monitored at 480.2 nm (Reddy et al., 2004).

2.6. Morphology

The shape and morphological examination of SLNs was observed by transmission electron microscopy (TEM). TEM of the nanoparticles was carried out at various magnifications (Morgagni 268D, Netherlands) in aqueous medium. The photo-micrographs were obtained after by sprinkling and drying the formulations on 3 mm

Forman (0.5% plastic powder in amyl acetate) coated copper grid (300 mesh) and the negatively staining with 4% uranyl acetate (Yadav et al., 2007).

2.7. Particle size, polydispersity index (PDI) and zeta potential

Suitably diluted suspensions of SLN-DOX and CBSA-SLN-DOX were separately filled in the chamber of laser diffraction particle size analyzer (DTS Ver. 4.10, Malvern Instruments, England). The average particle size and PDI were determined at a fixed angle of 90° at 25 °C after diluting the samples with deionized water via photon correlation spectroscopy. The zeta potential was determined by laser doppler anemometry using a Malvern Zetasizer (DTS Ver. 4.10; Malvern Instruments). SLNs were dispersed in PBS (pH ~7.4), placed in the electrophoretic cell where an electric field of 23.2 V/cm was applied and the zeta potential was measured.

2.8. In vitro release study

In vitro release of SLN-DOX and CBSA-SLN-DOX was estimated using dialysis tube diffusion technique. Ten milligrams of formulations were separately were suspended in PBS (pH 7.4; 2 mL) and placed into a dialysis sac (MWCO 1000 Da; Himedia, India). The dialysis tube was placed into 50 mL of aqueous recipient medium of PBS. The medium was continually stirred at 100 rpm at 37 ± 2 °C throughout the study. Aliquots were withdrawn at specific time-intervals (1, 2, 4, 8, 24, 48, 72, 96, 120, 144 h) and replaced with equal volume of fresh PBS. The samples were then assayed by HPLC to quantify the drug release. Similar, study was performed by adding 1% albumin along with PBS.

2.9. Cellular uptake

Cellular uptake studies were carried using fluorescence activated cell sorters (FACS) instrument (BD Biosciences FACS Aria, Germany) on brain capillary endothelial cells (BCs) and HNGC1 cells, according to a procedure reported elsewhere with modifications (Huang et al., 2002; Kolhe et al., 2003). HNGC1 cell lines were obtained from National Center for Cell Sciences, Pune, India. The cells were cultured in DMEM (Himedia, India) supplemented with 10% heat-inactivated fetal bovine serum (FBS), streptomycin (100 units/mL), 3 mmol/L L-glutamine at 37 °C in a 5% CO_2 humidified incubator. Aliquots (BCs and HNGC1 cells) were seeded at 2×10^5 cells/well in 12 well plates (Sigma, Germany) containing fresh DMEM + 10% FBS and suspended for 24 h in humidified incubator at 37 °C with 5% CO_2 atmosphere. Subsequently the media was removed and replaced with fresh DMEM. DOX in either free form or SLN-DOX, CBSA-SLN-DOX and free CBSA (1 mg/mL) + CBSA-SLN-DOX was added to separate wells. The formulations were added in a concentration of 50 ng equivalent of DOX. Moreover, to rule out that DOX uptake effects were due to concentration differences of various formulations, adequate dilutions of the formulations were done with PBS. After 1, 4 and 8 h of *in vitro* incubation, cells were washed with ice-cold PBS, trypsinized (0.1%, w/v), then palletized via centrifugation ($1000 \times g$) to remove the trypsin and finally resuspended in PBS. The cell-associated fluorescence profiles of DOX were quantified by fluorescence activated cell sorters (FACS) instrument (BD Biosciences FACS Aria, Germany).

2.10. Fluorescent microscopy of nanoparticle binding/uptake

BCs and HNGC1 cells were seeded at 2×10^4 cells/well in 24 well plates and allowed to adhere for 48 h at 37 °C under 5% CO_2 and the media was replaced with fresh DMEM. Subsequently, DOX, SLN-DOX, CBSA-SLN-DOX and free CBSA (1 mg/mL) + CBSA-SLN-DOX containing 2 μM equivalents of DOX were added in separate wells. The formulations were incubated of 5 h, the cells were washed with PBS (pH 7.4) and fixed using 3.7% paraformaldehyde. The slides were mounted on fluorescent microscope (Nikon, Japan) and visualized.

2.11. Cytotoxicity study

The inhibition of cell growth as a function of conjugation of ligand was determined by *in vitro* incubation of cells with plain DOX and its various formulations. The study was performed by 3-(4,5-dimethylthiazol-2yl)-2,5-diphenyl tetrazolium bromide (MTT) based assay (Agarwal et al., 2009a,b; Kolhe et al., 2003). HNGC1 cells were cultured following the same protocol reported for cellular uptake. Exponentially growing HNGC1 cells were harvested during logarithmic growth phase in 96-well plates (2×10^5 cells/well) and incubated for 24 h at 37 °C in a 5% CO_2 humidified atmosphere. The cells were treated with plain DOX, SLN-DOX, CBSA-SLN-DOX and free CBSA (1 mg/mL) + CBSA-SLN-DOX. DMEM containing a series of concentration gradient (10.0–0.01 μM) of DOX formulations were simultaneously incubated to each corresponding well and incubated for 72 h. Further, MTT solution (10 mg/mL) was added to each well and the incubation was continued for an additional 4 h, assisting MTT to be reduced by viable cells with the formation of purple formazan crystals. The formazan crystals were dissolved in DMSO and sonicated for 10 min. The absorbance of individual wells was measured at 570 nm via an ELISA plate reader.

2.12. In vitro transendothelial transport study

Brain capillary endothelial cells (BCs) and astrocytes cells were co-cultured at a density of 2×10^5 and 2.4×10^5 cells/well on the lower side and upper side respectively in polycarbonate 24 well cell culture insert with 1 μm-diameter microporous PET membrane. The cells were cultured for three days at 37 °C in 10% CO_2 and examined for 100% confluency. Two hundred microliter of plain, DOX, SLN-DOX, CBSA-SLN-DOX and free CBSA (1 mg/mL) + CBSA-SLN-DOX formulations in Ringer-HEPES solution were added to different wells of the luminal compartment. The concentration of DOX in all the wells was 20 μg/mL. At various time intervals, cells and aliquots in the abluminal side were isolated. The cells were disrupted using Triton X-100 (5%; 250 μL) and the suspension was centrifuged (10,000 rpm; 30 min). The supernatant was withdrawn and the DOX associated fluorescent intensity (Perkin–Elmer LS55 Luminescence Spectrometer, Shelton, CT) was measured at an excitation/emission wavelength of 475/580 nm.

2.13. In vivo pharmacokinetic and biodistribution studies

In vivo studies were performed with prior permission and in accordance with standard institutional guiding principles specified by the Institutional Animals Ethical Committee. The implications of *in vivo* studies were further correlated using various pharmacokinetic and pharmacodynamic parameters. The animals (Balb/c mice; 20–25 g; either sex) were fasted overnight with access to water ad libitum.

The mice were divided into four groups (18 animals in each group). The animals of the first group were injected with plain DOX (5.0 mg/kg body weight) into their tail vein; second and third group of mice was administered SLN-DOX and CBSA-SLN-DOX, respectively via tail vein (dose equivalent to 5.0 mg/kg body weight of DOX) (Gulyaev et al., 1999). The mice of fourth group were kept as control. Blood samples were obtained from retro-orbital plexus of animal's eye at 0.16, 0.5, 1.0, 2.0, 3.0, 5, 8, 12, 18, 21 and 24 h intervals in heparinized tubes. Blood was withdrawn from adequately marked six animals of each group for 0–2 h intervals and subsequently, they were sacrificed by cervical dislocation. The organs

(brain, heart, kidney, liver, and spleen) were excised, weighed and stored at −80 °C until assay. Further, blood was withdrawn from other six animals ($n = 6$) of each group for 2–8 h intervals and subsequently they were sacrificed and different organs were isolated. Same protocol was followed for last six animals of each group for 8–24 h intervals. This method was applied because only about 1.75 mL blood is present in 25 g mice and it is not enough to facilitate withdrawal of blood for 24 h time period from the same animal.

The blood samples were centrifuged at 3000 rpm for 15 min to separate RBCs and the serum was collected with the help of micropipette. One hundred microliter of serum was filtered through 0.22 μm-membrane filter (Pall Gelman Sciences, USA) and 100 μL of 10% (w/v) trichloroacetic acid (TCA) was added. Simultaneously, the organs were homogenized to separate the tissues, vortexed for 45 s, and kept aside for 30 min. The homogenates were then treated with 100 μL of 10% TCA solution. Further, the serum and tissue homogenates previously admixed with TCA were vortexed for 1 min, 500 μL of methanol was added and subsequently centrifuged at 3000 rpm for 15 min. The supernatant was filtered through a 0.22-μm membrane, collected in HPLC vials (Himedia, India) and quantified for DOX. Quantification of DOX in serum and various tissues was performed by HPLC (Reddy et al., 2004).

2.14. Hematological study

Balb/c mice were used for determination of hematological parameters. Plain DOX (first group), SLN-DOX (second group), and CBSA-SLN-DOX (third group) formulations were administered in a dose equivalent to 5 mg/kg weight of DOX every day up to 7 days. Fourth group of animals was kept as control. For hematological evaluations, the total white blood corpuscles (WBC), red blood corpuscles (RBC), platelets count and hemoglobin (Hb) content were determined at 8th day using a semi-automated blood cell counter with digital display (Sysmex cc-130, Toa Medical Electronics Ltd., Japan).

2.15. Evaluation of nephrotoxic and hepatotoxic effect

Balb/c mice of either sex were divided into 4 groups of six animals in each group. Animals of groups I, II, and III were i.v. administered injected a single dose of plain DOX, SLN-DOX and CBSA-SLN-DOX, respectively via tail vein. The drug either in plain solution or encapsulated in nanoparticles was given in a concentration equivalent to 5 mg/kg body weight. Animals of group IV served as control. After 72 h of administration of different formulations, blood samples were collected through retro-orbital plexus of the eye. The samples were subjected to centrifugation at 3500 rpm for 20 min and the serum was collected.

Serum level of urea was determined by urease–glutamate dehydrogenase method and creatinine by the modified Jaffe's method using the diagnostic kits of Agappe Diagnostic India Pvt. Ltd. (Ajith et al., 2008). Serum glutamine pyruvic transaminase (SGPT), aspartate aminotransferase (AST) and alkaline phosphatase (ALP) activity in the serum were determined using commercially available test kits from Randox Laboratories Ltd. (UK) (Injac et al., 2008).

2.16. Statistical analysis

The statistical results obtained were stated as mean ± SD and the analysis was carried by one-way analysis of variance (ANOVA) using GraphPad InStat™ software (GraphPad Software Inc., San Diego, CA). A probability level of $p < 0.05$ was considered to be significant.

3. Results and discussion

3.1. Preparation of solid lipid nanoparticles (SLN-DOX)

SLNs were prepared by melt emulsification followed by homogenization and were then lyophilized. The technique incorporates rapid movement of organic solvent from the solvent–lipid phase into water (containing 2% (w/v) Poloxamer 188). Subsequently, the organic solvent vaporizes that facilitates solidification and rigidization of lipid particles. Poloxamer 188 was used as surfactant for the formation of SLNs. Stearic acid was incorporated to offer carboxylic acid tailored functionalities on SLNs, which were further employed in conjugation of a ligand (Fig. 1). Presence of O–H stretch of alcohol at 3130.06 cm^{-1}, C=O stretch at 1739.16 cm^{-1} and C–O stretch at 1086.16 cm^{-1} in the FTIR spectrum established the presence of terminal carboxylic acid (–COOH) functionalities of stearic acid for ligand conjugation (Fig. 2). Furthermore the presence of –NH stretch at 3474.56 cm^{-1} and also weak combination and overtone bands between 2100 and 1700 cm^{-1} of aromatic hydrocarbons confirms the presence of DOX in the nanoparticulate formulation. In addition, the formulation of SLNs with –COOH functionalities placed on the surface was proved by ^1H NMR spectroscopy. A peak between $\delta = 10.9$ and 11.1 ppm depict hydroxyl groups of carboxylic acid (–OH groups of –COOH of stearic acid). Further the peaks between $\delta = 1.1$–1.8 ppm and 2.2–3.8 ppm potray –CH skeleton of tristearin and stearic acid (Fig. 3).

3.2. Preparation of cationic bovine serum albumin (CBSA)

The FTIR spectroscopy illustrated characteristic peaks of BSA at 3342.17 cm^{-1} (N–H stretch), 1648.25 cm^{-1} (C=O stretch) and 1024.64 cm^{-1} (C–O bending). Peaks in the FTIR spectrum of CBSA were of higher intensity though at the similar wavelength. This may be attributed to presence of an additional $–CH_2–CH_2–NH_2$ group in CBSA imparted during cationization (Supplementary Data). IEF illustrated pI of BSA to be between 3.5 and 4.5 and which augmented to values between 8 and 9 upon cationization (Fig. 4a). The results are in line with previous studies which report CBSA to serve as brain targeting agent should have pI between 8 and 9 (Thole et al., 2002). Further, SDS-PAGE shows that molecular weight remained unaltered for CBSA and only a minimal dimerization was observed (Fig. 4b). This is crucial because uncontrolled cationization may lead to generation of high molecular weight aggregates.

3.3. Preparation of CBSA conjugated DOX loaded SLNs (CBSA-SLN-DOX)

Synthesis of CBSA conjugated SLNs was confirmed by FTIR and NMR. Addition of CBSA in presence of NHS and EDAC lead to amide (–CONH–) bond formation between amine ($–NH_2$) groups of CBSA and carboxylic acid (–COOH) terminal functionalities on the surface of SLN-DOX. The presence of peaks depicting N–H stretch at 3450.12 cm^{-1}, C=O stretch at 1706.40 cm^{-1} and C–O stretch 1460.42 cm^{-1} confirmed the amide bond formation and hence conjugation between SLNs and CBSA (Fig. 5). NMR spectra reveals a new peak at $\delta = 8.0$–8.4 ppm (–NH–) and disappearance of a peak between $\delta = 10.9$ and 11.1 ppm (–OH group of –COOH) which further confirms amide bond formation between carboxylic groups of SLNs and amine groups of CBSA (Fig. 6). Other peaks obtained in the NMR were similar to those seen in spectra of plain carboxylic acid terminated SLNs. In the present study, the % coupling efficiency of CBSA on the surface of SLNs was 22.9%.

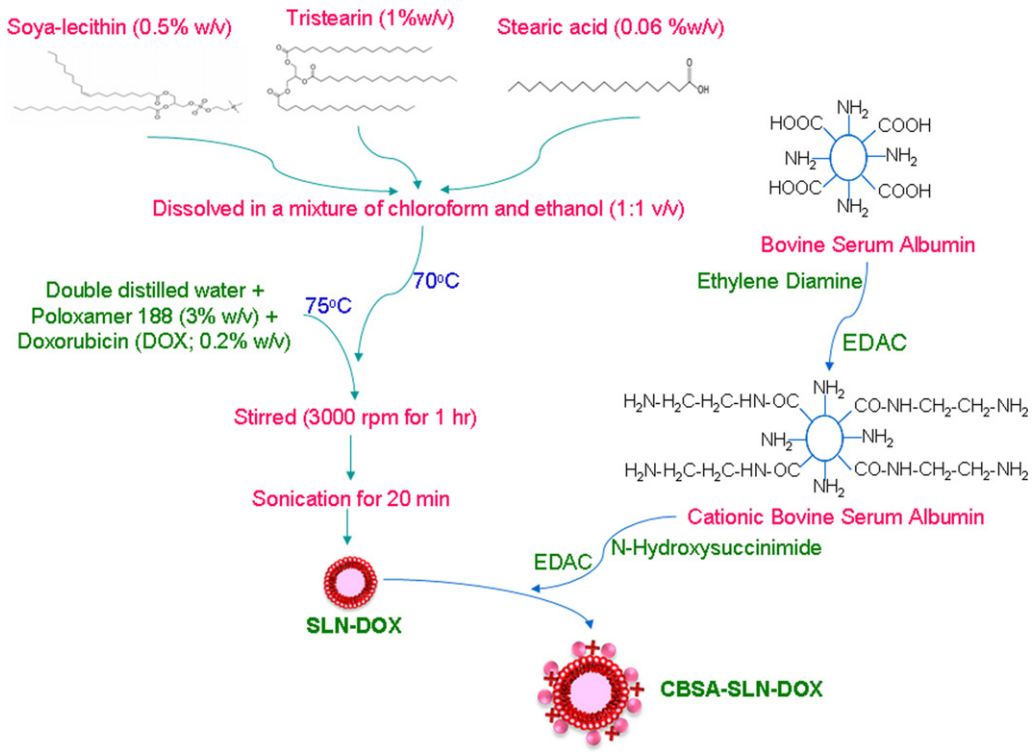

Fig. 1. Schematic representation of method for preparation of SLN-DOX and CBSA-SLN-DOX.

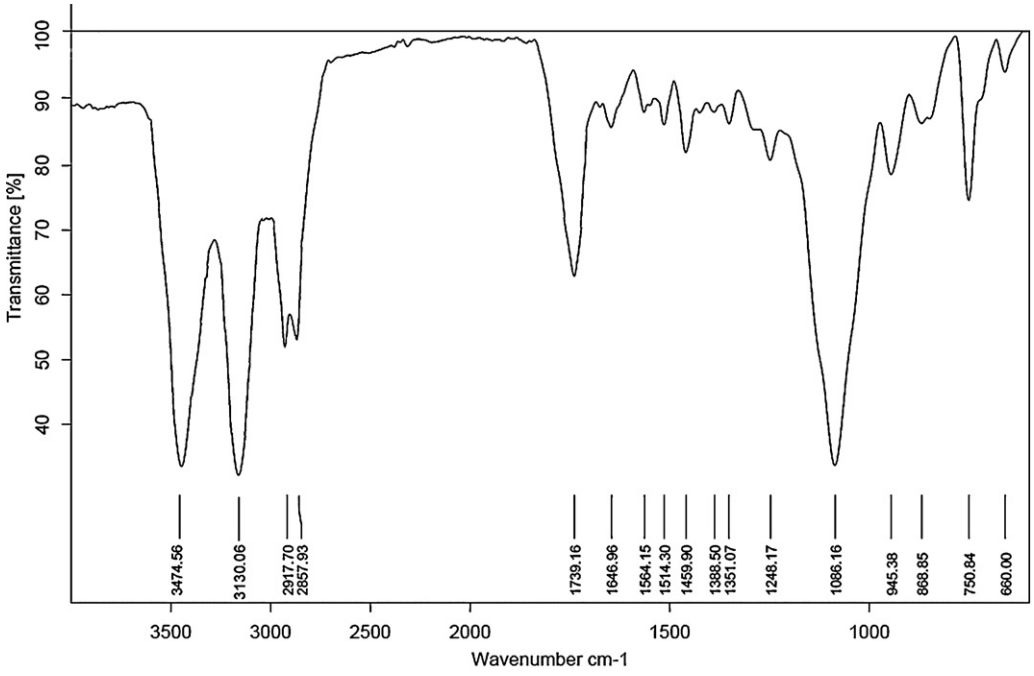

Fig. 2. FTIR spectrum of SLN-DOX.

Table 1
Comparison of various physicochemical parameters of SLNs.

Formulation	Particle size (nm)	PDI	Zeta potential (mV)	Entrapment efficiency (%)
SLN-DOX*	80.9 ± 1.7	0.082 ± 0.008	−13.5 ± 0.5	45.3 ± 0.6
CBSA-SLN-DOX*	95.1 ± 1.8	0.073 ± 0.011	+14.1 ± 0.7	42.5 ± 0.5

Mean ± SD ($n = 6$; $p \leq 0.05$).
* Significant difference between SLN-DOX and CBSA-SLN-DOX.

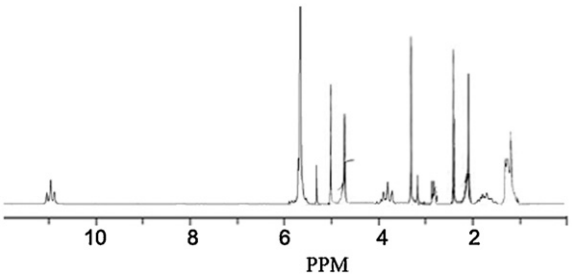

Fig. 3. NMR spectrum of SLN-DOX.

3.4. Drug content

Entrapment efficiency of doxorubicin in SLN-DOX and CBSA-SLN-DOX was 45.3 ± 0.6% and 42.5 ± 0.5%, respectively (Table 1). The % payload of DOX in SLN-DOX and CBSA-SLN-DOX was 5.81% and 5.45%, respectively. Slightly lower loading was obtained in CBSA-SLN-DOX possibly due to the loss of surface adsorbed drug during conjugation with CBSA. The results are in line with earlier reports (Soni et al., 2006).

3.5. Morphology

TEM photomicrographs reveal spherical shape of SLNs (Fig. 7). Photomicrographs also illustrate nanoparticulate range and a slight augmentation in size upon conjugation of a ligand on the surface of SLNs.

3.6. Particle size, polydispersity index (PDI) and zeta potential

The average size of SLN-DOX and CBSA-SLN-DOX was 80.9 ± 1.7 nm (PDI of 0.082 ± 0.008) and 95.1 ± 1.8 nm (PDI of 0.073 ± 0.011), respectively. The nanoparticles of such small size were produced possibly because sonication time for 20 min imparts increased energy transfer to the dispersion medium where by the

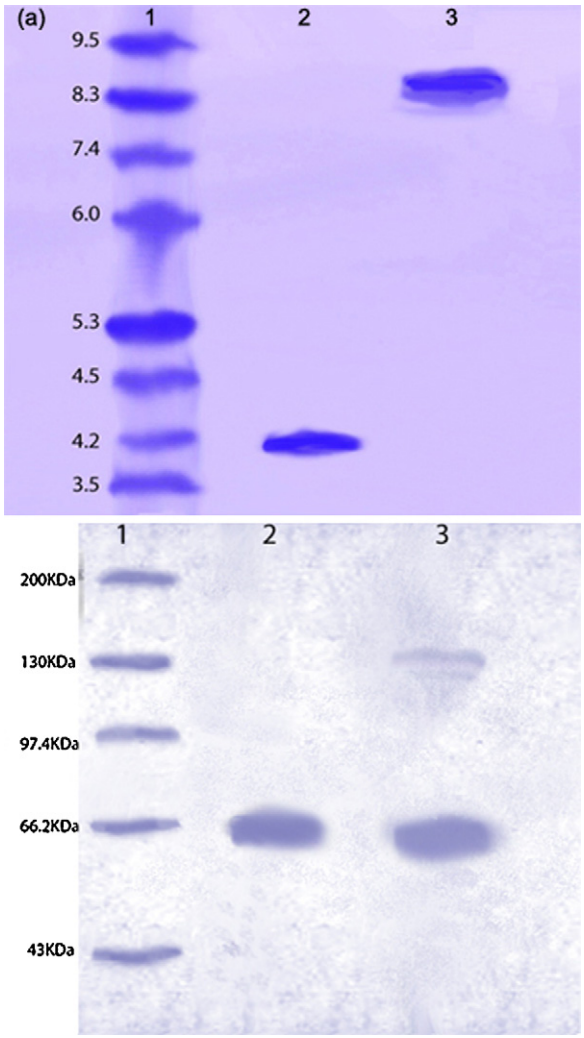

Fig. 4. (a) IEF and (b) SDS-PAGE diagram of marker (lane 1), BSA (lane 2), and CBSA (lane 3), respectively.

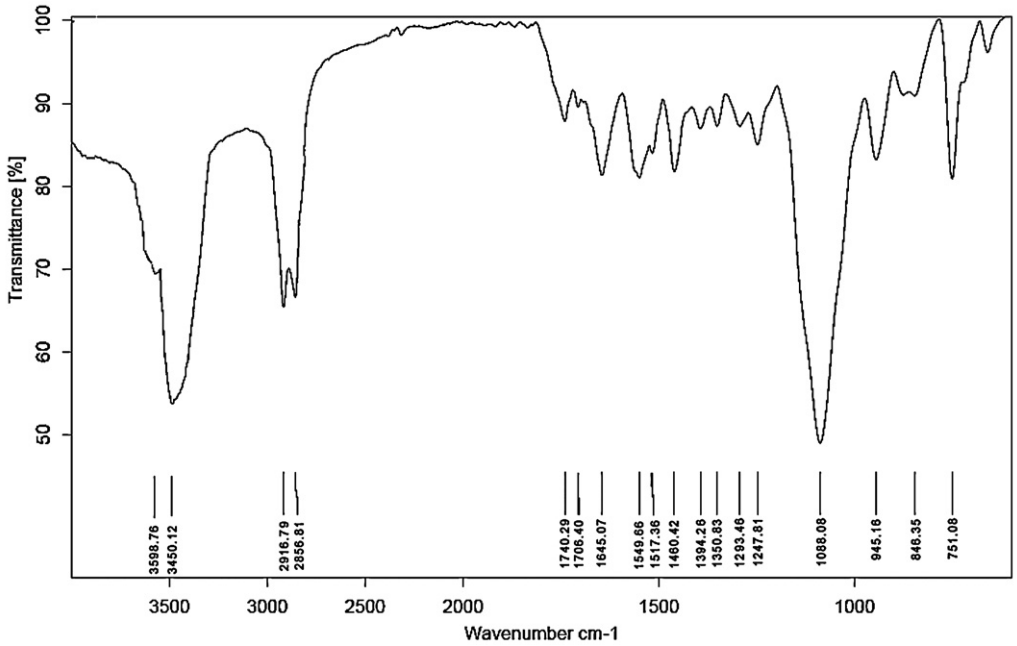

Fig. 5. FTIR spectrum of CBSA-SLN-DOX.

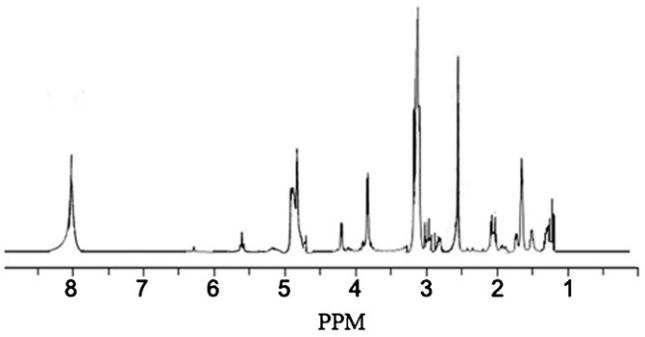

Fig. 6. NMR spectrum of CBSA-SLN-DOX.

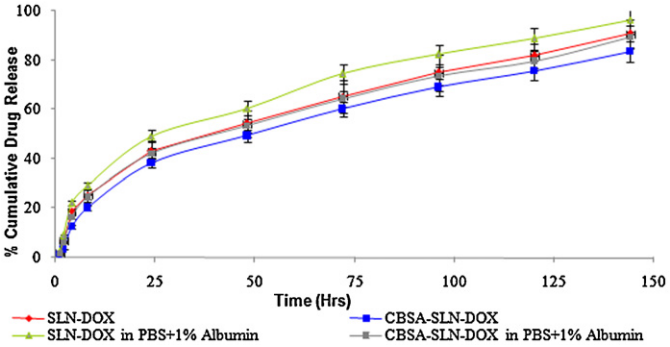

Fig. 8. *In vitro* drug release of DOX in PBS, pH 7.4 and PBS + 1% albumin from SLN formulations ($n = 6$; $p \leq 0.05$ (significant difference between SLN-DOX and CBSA-SLN-DOX)).

lipid solution was dispersed into smaller droplets and hence the size was reduced. The alteration in size is possibly a consequence of ligand conjugation (Table 1). Furthermore, the results are in agreement with TEM studies that confirm submicron range and an increase in size upon attachment of a ligand.

Zeta potential of SLN-DOX was found to be -13.5 ± 0.5 mV and augmented to 14.1 ± 0.7 mV upon ligand conjugation. Negative charge on plain SLNs may be bestowed to carboxylic groups ($-COO^-$) present on their surface. These were subsequently replaced with terminal amine (NH_2) groups upon conjugation of CBSA and this lead to an alteration in zeta potential to a positive value.

3.7. *In vitro* release study

In vitro the formulations displayed a biphasic pattern and an initial burst release viz $20.3 \pm 0.5\%$ and $25.4 \pm 0.6\%$ of DOX was obtained from CBSA-SLN-DOX and SLN-DOX, respectively in the PBS until the end of 8th hour (Fig. 8). A possible reason that may be accounted is the fast release of drug entrapped in the outermost stratum or adsorbed on the surface of the SLNs. Further, the cumulative DOX release from CBSA-SLN-DOX and SLN-DOX was $83.5 \pm 1.5\%$ and $90.7 \pm 1.8\%$, respectively at the end of 144 h. This sustained and prolonged release of drug molecules observed was mainly due to diffusion of drug through the lipid matrix of the SLNs. The results also depict that coupling of CBSA impedes the drug release from the SLNs. This may possibly be due to structural integrity conferred by CBSA thus providing a diffuse double layer barrier and offering a steric barrier to diffusion of drug. The results are in accordance to previously reported data (Soni et al., 2006). Further, an augmented cumulative drug release was seen in PBS (0.1 M; pH 7.4) + 1% albumin when compared to PBS (0.1 M; pH 7.4). The rationale that may be ascribed is affinity of DOX for albumin (protein binding) and modified physiological conditions upon addition of albumin.

3.8. Cellular uptake

Flow cytometry has been used for quantitative estimation of DOX uptake in the cells. The uptake profile of SLNs as a function of CBSA conjugation was executed on BCs and HNGC1 tumor cell lines. In BCs the percent fluorescent cells, 1 h post incubation of plain DOX, SLN-DOX, CBSA-SLN-DOX, and free CBSA + CBSA-SLN-DOX in BCs was $7.3 \pm 0.2\%$, $10.3 \pm 0.4\%$, $28.9 \pm 0.8\%$, and $8.7 \pm 0.4\%$, respectively (Fig. 9a). Cellular uptake augmented with time ($p \leq 0.05$), which is obvious from the increase in % fluorescent cells to $25.6 \pm 0.7\%$, $39.8 \pm 1.1\%$, $95.4 \pm 1.9\%$, and $34.8 \pm 1.0\%$, respectively after 8 h. Accordingly in HNGC1 tumor cell lines, after 1 h of incubation of free DOX, SLN-DOX, CBSA-SLN-DOX, and free CBSA + CBSA-SLN-DOX the percent fluorescent cells were $8.1 \pm 0.3\%$, $12.4 \pm 0.5\%$, $32.4 \pm 0.9\%$, and $10.9 \pm 0.5\%$, respectively. The value increased to $28.3 \pm 0.6\%$, $43.2 \pm 0.8\%$, $99.7 \pm 2.1\%$, and $39.1 \pm 0.6\%$, respectively after 8 h (Fig. 9b). The higher uptake of CBSA-SLN-DOX was possibly due to CBSA residues tethered on the surface of SLNs when compared to SLN-DOX ($p < 0.005$). This foremost cellular entry may be ascribed to adsorption mediated endocytosis mechanism facilitated by CBSA. In contrast incubation of free CBSA along with CBSA-SLN-DOX led to distinctly reduced entry both in ECs and HNGC1 tumor cell lines. This may be endorsed to competitive inhibition of CBSA tethered SLNs with free CBSA. Free CBSA preferentially gained access into the cells and therefore little entry of CBSA-SLN-DOX was observed. The results are lined up with earlier studies (Storm et al., 2002).

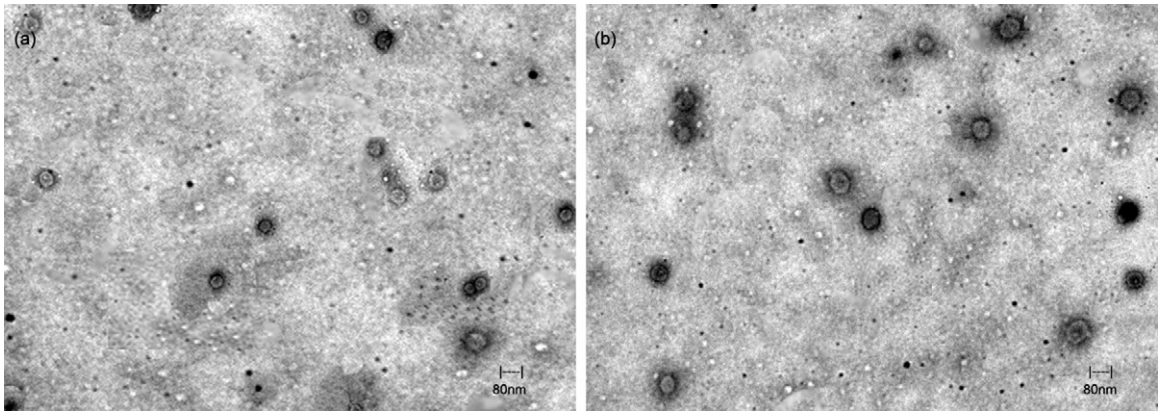

Fig. 7. TEM photomicrographs of (a) SLN-DOX and (b) CBSA-SLN-DOX.

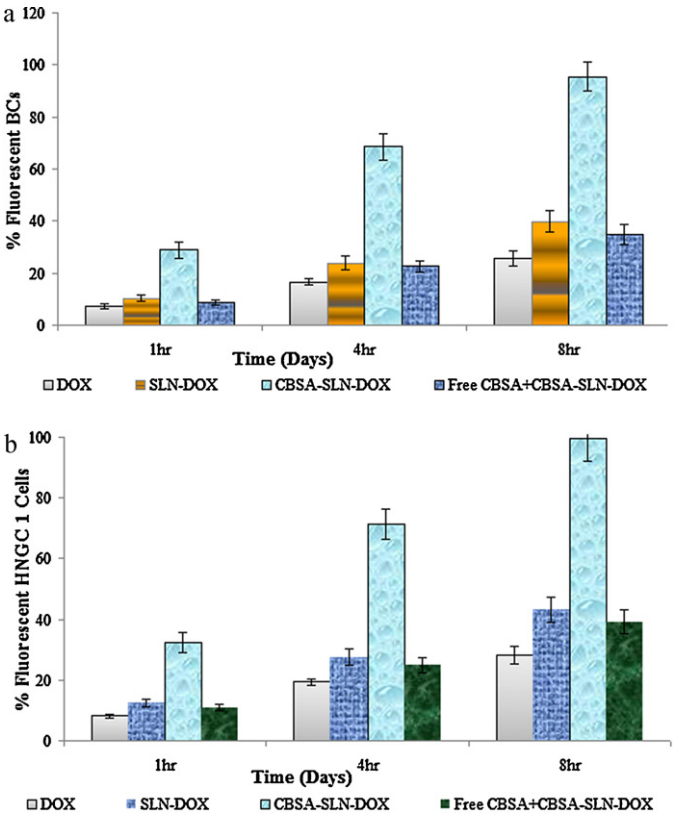

Fig. 9. Cellular uptake of DOX in (a) BCs and (b) HNGC1 cell lines from plain DOX, SLN-DOX, CBSA-SLN-DOX and free CBSA + CBSA-SLN-DOX. Mean ± SD ($n = 6$; $p \leq 0.05$ (significant difference between plain DOX vs. SLN-DOX and CBSA-SLN-DOX; significant difference between SLN-DOX and CBSA-SLN-DOX)).

Further, some uptake was visualized with SLN-DOX but less than CBSA-SLN-DOX and may be ascribed to non-specific entry mediated by diffusion/endocytosis/phagocytosis. In addition, it may be possible that plain DOX alone as well as SLN-DOX were not internalized but adhered on to the surface of cells and thereby elucidating some fluorescence.

It is imperative to state that although CBSA-SLN-DOX facilitates higher cellular uptake in BCs, *in vivo* the ligand tethered formulation would promptly experience transcytosis thus evading the possibility of marked cytotoxic effect on BCs as compared to SLN-DOX or plain DOX itself. Additionally, *in vivo* once endocytosed in the tumor cells, CBSA-SLN-DOX would be entrapped in the tumor vasculature via enhanced permeation and retention effect. Thus, a higher cytotoxic action may possibly be observed on the tumor mass.

3.9. Fluorescent microscopy

Analogous to the results of quantitative cellular uptake studies reported above, fluorescent photomicrographs showed higher uptake of CBSA-SLN-DOX in BCs as well as in tumor cells, followed by SLN-DOX > CBSA + CBSA-SLN-DOX > plain DOX at equivalent concentrations of DOX (Figs. 10 and 11).

3.10. Cytotoxicity study

In vitro cell survival fraction of HNGC1 cells after incubation with DOX, SLN-DOX, CBSA-SLN-DOX and CBSA + CBSA-SLN-DOX were analyzed using MTT assay. HNCG1 cell lines were incubated with doses ranging from 10.0 to 0.01 μM. The result of the cell inhibition assay exhibited considerable differences. In similarity to results of cellular uptake CBSA-SLN-DOX exhibited the highest percent cell growth inhibition compared to plain DOX or SLN-DOX. In all the formulations nearly no influence to the viability of cells was seen when the equivalent concentration of DOX was below 1 μM/mL and the cell viabilities obtained were all above 95% (Fig. 12).

As the equivalent concentration of DOX was augmented beyond 1 μM/mL, the cytotoxic effect was sort out as plain DOX < free CBSA (1 mg/mL) + CBSA-SLN-DOX < SLN–DOX < CBSA-SLN-DOX. Experiments performed on xenografts model clearly illustrate a dose dependent cytotoxic activity that is a decrease in survival fraction with increase in concentration of drug. Probably, the cytotoxic action of drug that intercalates with DNA depends upon entry of drug in the cell and not merely by its presence in the surrounding milieu of a cell. CBSA conjugation facilitated maximum intracellular entry of CBSA-SLN-DOX via adsorption mediated endocytosis. Subsequently slow and sustained release of DOX lead to a significantly higher cytotoxic action as compared free DOX or SLN-DOX. The cytotoxic effect via plain SLNs (SLN-DOX) was less than ligand conjugated SLNs possibly due to their entry in absence of any active transport mechanism and mediated merely by passive diffusion. Similar results have been obtained in earlier studies. Yadav et al. (2010) illustrated the cytotoxic effect of chondritin sulfate (CS) anchored nanoparticles to be greatest as compared to non-ligand conjugated nanoparticles or plain drug. This was ascribed to ligand-receptor activity between CS and its receptors present on the surface of tumor cells, which possibly promoted their augmented internalization. In a similar study performed on drug-resistant human breast cancer cells, Wong et al. revealed 8-fold higher cytotoxic action of doxorubicin loaded in a polymer–lipid hybrid nanoparticle system as compared to plain doxorubicin solution (Wong et al., 2006).

Further, a 100% cell inhibition was perceived from all the formulations when the equivalent concentration of free DOX or its SLNs formulations was 100 μM/mL or more. A possible reason may be entry of adequate amount of DOX inside the cell from all the formulations at this concentration during a fairly long incubation time of 72 h.

3.11. In vitro transendothelial transport study

Transcytosis ability of plain DOX, SLN-DOX, CBSA-SLN-DOX and free CBSA (1 mg/mL) + CBSA-SLN-DOX was studied on a coculture of BCs and astrocytes (Fig. 13). Their permeability coefficient (Pe) were 0.8×10^{-6} cm/s, 1.9×10^{-6} cm/s, 2.5×10^{-5} cm/s, and 1.1×10^{-6} cm/s, respectively. The results point that maximum transendothelial transport was obtained in case of CBSA-SLN-DOX. This may be attributed to ability of cationic protein conjugated SLNs to undergo adsorptive-mediated transcytosis across the BCs. Transendothelial flux was less for free CBSA + CBSA-SLN-DOX, possibly due to presence of free CBSA which competitively inhibited the movement. This further verifies that the transendothelial movement was mediated by CBSA.

3.12. In vivo pharmacokinetic and biodistribution studies

Circulation life time, pharmacokinetics as well as therapeutic efficacy of DOX was immensely altered upon entrapment in SLNs and conjugation of a ligand. Fig. 14 represents the plasma profiles of various DOX formulations after single i.v. injection in Balb/c mice. The resulting pharmacokinetic parameters were determined and are shown in Table 2. The initial C_{max} obtained after injection of DOX loaded in SLNs was slightly lower than plain DOX. However, DOX was detected in the serum until the end of 24 and 21 h after administration of CBSA-SLN-DOX and SLN-DOX, respectively, and only for 8 h in case of plain DOX solution. Furthermore, the serum AUC_{0-24}, $AUC_{0-inf,}$ $AUMC_{0-t}$ and $AUMC_{0-inf}$ of

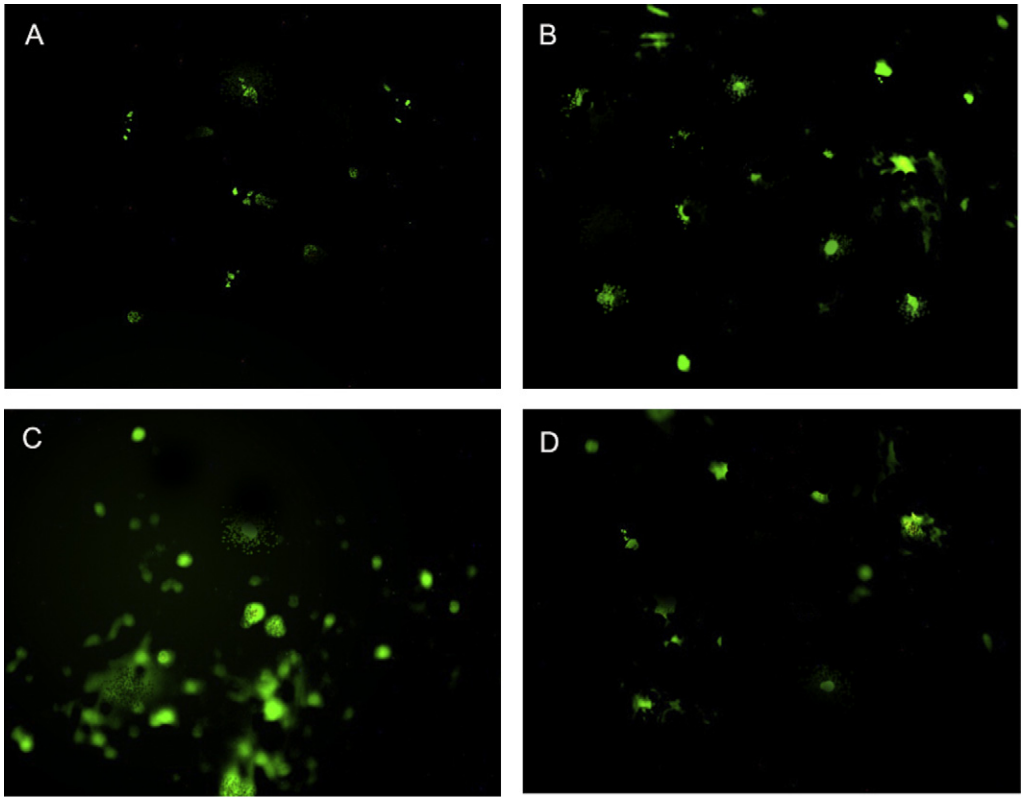

Fig. 10. Fluorescent photomicrographs of uptake of DOX in BCs from plain DOX, SLN-DOX, CBSA-SLN-DOX and CBSA + CBSA-SLN-DOX.

Table 2
Pharmacokinetic parameters in serum of Balb/c mice.

Parameters	Plain DOX	SLN-DOX	CBSA-SLN-DOX
C_{max} (μg)	4.87	4.15	3.95
K_{el}	0.47	0.15	0.13
Cl_t (mL/h)	465.12	163.18	134.70
AUC_{0-t} (μg h/mL)	10.75	30.64	37.12
AUC_{0-inf} (μg h/mL)	10.96	31.11	39.33
$AUMC_{0-t}$ (μg h^2/mL)	20.85	203.12	293.15
$AUMC_{0-inf}$ (μg h^2/mL)	23.02	216.16	363.12
$T_{1/2}$ (h)	1.48	4.65	5.29
MRT (h)	2.09	6.95	9.23

CBSA-SLN-DOX was 1.21, 1.26, 1.44 and 1.68 folds higher than SLN-DOX and 3.45, 3.59, 14.06 and 15.77 folds higher than plain DOX, respectively. The results clearly indicate long circulation property of SLNs with ligand conjugated formulation having the greatest circulation duration. The studies are in line with previous reports that stated CBSA to have favorable pharmacokinetic properties with a longer serum half-life (Bickel et al., 2001). The mean residence time (MRT) of CBSA-SLN-DOX, SLN-DOX and plain DOX was 9.23, 6.95 and 2.09 h, respectively. Additionally, the half-life ($t_{1/2}$) of CBSA-SLN-DOX, SLN-DOX and plain DOX was 5.29, 4.65, and 1.48 h, respectively. These data also support extended residence time and sustained release profile of the drug loaded in SLNs in body as compared to free DOX and the maximum being for CBSA conjugated formulation. The blood level of DOX was sustained to a greater extent in case of CBSA-SLN-DOX than SLN-DOX possibly due to double barrier effect to drug diffusion upon ligand conjugation (Soni et al., 2006). Furthermore, the high Cl_t and K_{el} of plain DOX as compared to DOX loaded in SLNs indicated their slow clearance from the body and may be conferred to encapsulation of drug in the nanoparticles. The data presented to this point clearly imply CBSA-SLN-DOX have markedly better bioavailability and apparently more prolonged retention in systemic circulation and the effect could not be achieved via pre-treatment of mice with SLN-DOX or plain DOX.

Organ distribution studies were conducted to explore the possible effectiveness of CBSA-SLN-DOX to deliver DOX to brain tissues at the same time bypass non-target tissues (spleen, kidney, heart, and liver). The biodistribution of DOX from plain DOX and its formulations in solid organs was determined at the same time points as the brain (2, 8 and 24 h) (Fig. 15).

After, 2 h of administration the content of DOX when injected as plain solution in kidney, liver, heart, spleen, and brain tissues was 37.15 ± 0.81 μg/g, 12.01 ± 0.37 μg/g, 6.12 ± 0.16 μg/g, 9.35 ± 0.28 μg/g, and 0.45 ± 0.04 μg/g, respectively. The data clearly suggests the greatest access of plain DOX to the kidney, which is its major clearance organ and uptake by liver/spleen, which are the organs rich in cells of RES. The data also illustrates the rationale of cardiotoxicity produced by the drug, the concentration being high in heart. Only a minimal concentration of DOX was detected in brain. DOX being hydrophilic in nature, the blood brain barrier acts as a major obstacle for delivery and further considerably impedes therapeutic effect. Moreover, the concentration of free DOX declined quickly in all the organs being undetectable in brain and kidney after 24 h of administration. This indicates rapid elimination/metabolism and clearance of drug from the body when administered as plain solution.

Encapsulation of DOX in plain SLNs resulted in an elevated concentration of DOX in liver and spleen and may be attributed to uptake of lipid particulates by mononuclear phagocytic system. A slight increase in DOX concentration in brain tissues was also observed. Undoubtedly, augmented dwell time of DOX in the systemic circulation upon entrapment in SLNs facilitated redistribution of drug to different organs. However absence of a targeting moiety lead to non-specific/non-selective distribution and hence the effect was not prominent.

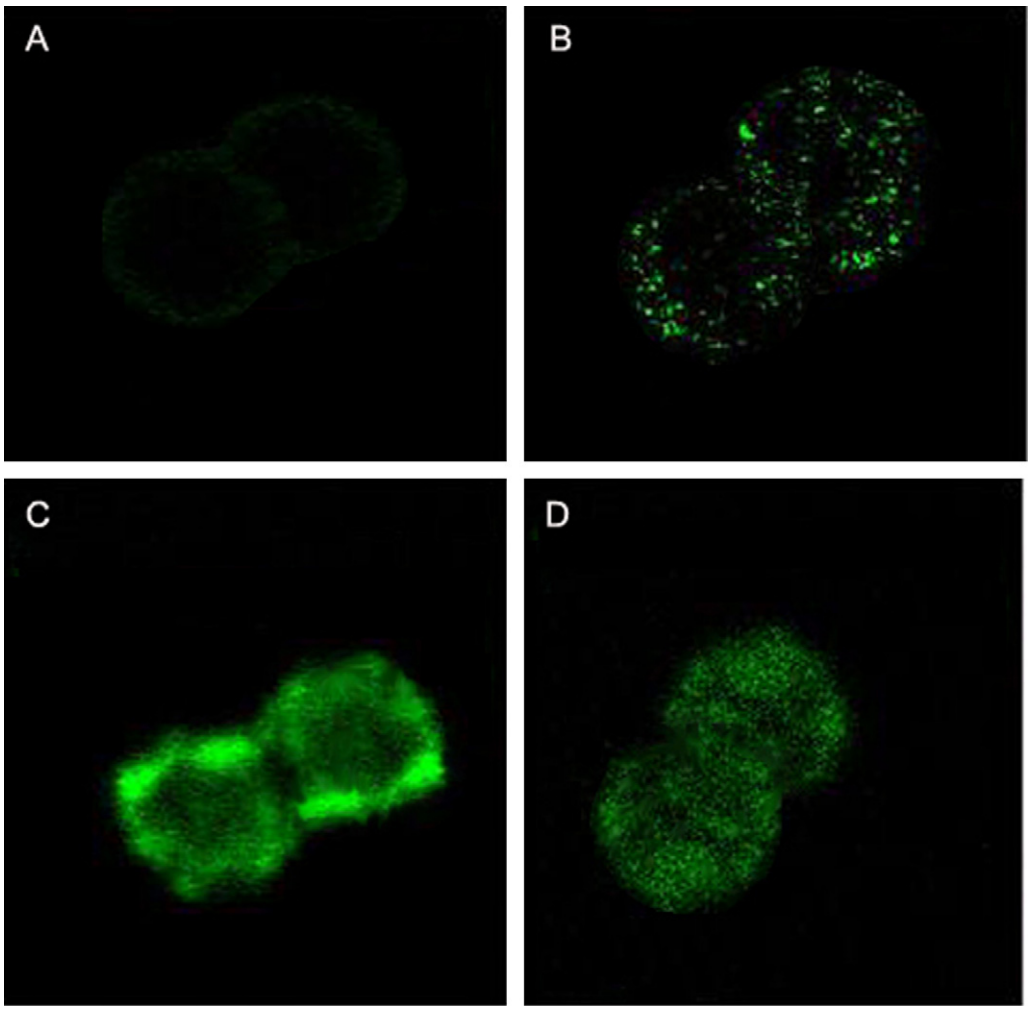

Fig. 11. Fluorescent photomicrographs of DOX uptake in the HNGC 1 cells from Plain DOX, SLN-DOX, CBSA-SLN-DOX and CBSA + CBSA-SLN-DOX.

In case of CBSA-SLN-DOX, the concentration of DOX in kidney, liver, heart, spleen, and brain tissues was 7.13 ± 0.41 μg/g, 9.92 ± 0.57 μg/g, 1.34 ± 0.05 μg/g, 8.54 ± 0.49 μg/g and 22.93 ± 0.68 μg/g, respectively after 2 h of administration. Hence after 2 h the DOX content with CBSA-SLN-DOX in brain was enhanced by 50.95 and 3.67 folds when compared to plain DOX and SLN-DOX. Additionally after 24 h no DOX and 9.76 ± 0.68 μg/g DOX was detected in brain tissues upon administration of plain DOX and CBSA-SLN-DOX, respectively. The results clearly suggest targeted delivery of drug to brain with CBSA conjugated SLNs. This may be attributed to CBSA conjugation that facilitates SLNs to pass across the blood brain barrier by adsorption mediated transcytosis (Lu et al., 2005, 2006).

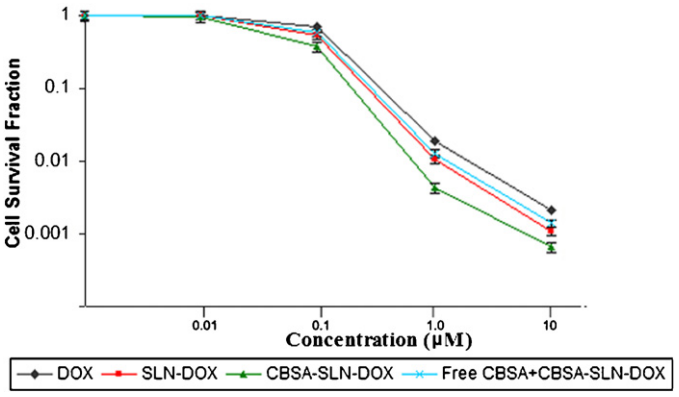

Fig. 12. Cytotoxicity study of plain DOX, SLN-DOX, CBSA-SLN-DOX and free CBSA + CBSA-SLN-DOX on HNGC 1 cell lines. Mean ± SD ($n = 6$; $p \leq 0.05$ (significant difference between plain DOX vs. SLN-DOX and CBSA-SLN-DOX; significant difference between SLN-DOX and CBSA-SLN-DOX)).

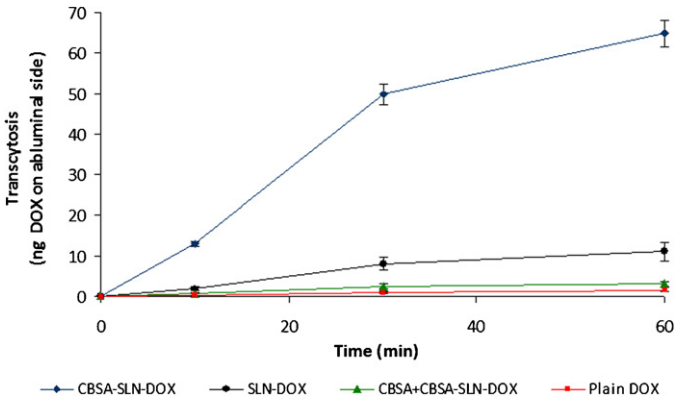

Fig. 13. Time dependent transcytosis of DOX across BCs from plain DOX, SLN-DOX, CBSA-SLN-DOX and free CBSA + CBSA-SLN-DOX. Mean ± SD ($n = 6$; $p \leq 0.05$ (significant difference between Plain DOX vs. SLN-DOX and CBSA-SLN-DOX; significant difference between SLN-DOX and CBSA-SLN-DOX)).

Table 3
Hematological parameters after administration of various nanoparticulate formulations.

Groups	WBC ($\times.10^3/\mu L$)	RBC ($\times10^6/\mu L$)	Hb (g/dL)	Platelet count ($\times10^3/\mu L$)
Control	7.3 ± 1.5	9.7 ± 0.6	17.2 ± 1.3	989.7 ± 37.5
Free DOX*	4.5 ± 0.4	6.4 ± 0.5	10.9 ± 0.8	761.2 ± 39.7
SLN-DOX*,a	6.8 ± 0.7	9.0 ± 0.8	16.3 ± 1.2	938.3 ± 42.4
CBSA-SLN-DOX*,a	7.1 ± 1.0	9.4 ± 0.5	16.8 ± 1.4	975.6 ± 38.2

$n = 6$; $p \leq 0.05$.
[a] Significant difference between SLN-DOX and CBSA-SLN-DOX.
* Significant difference between free DOX vs. SLN-DOX and CBSA-SLN-DOX.

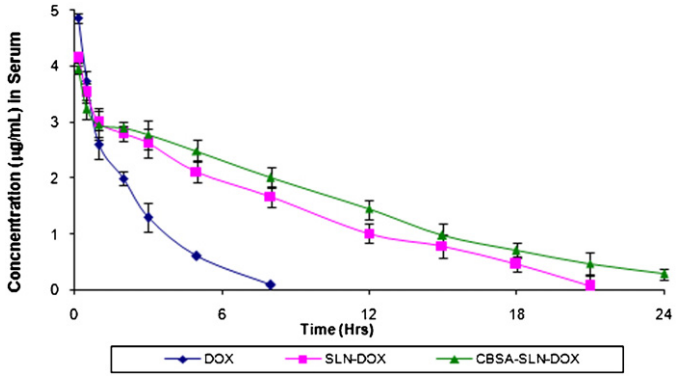

Fig. 14. Serum concentration of DOX obtained from plain DOX, SLN-DOX and CBSA-SLN-DOX at various time intervals. Mean ± SD ($n = 6$; $p \leq 0.05$ (significant difference between plain DOX vs. SLN-DOX and CBSA-SLN-DOX; significant difference between SLN-DOX and CBSA-SLN-DOX)).

Adding up, the RES uptake of CBSA-SLN-DOX was only slightly higher than plain DOX but less than SLN-DOX. This may possibly be due to presence of CBSA that has high affinity to brain tissues as compared to other organs (liver, heart, and lung). Moreover conjugation of protein ligand provided some surface hydrophilicity to SLNs that further helped to evade uptake of formulation by macrophage cells of liver and spleen. An imperative aspect was the noteworthy reduction in distribution of DOX to heart by CBSA-SLN-DOX indicating their prospective in diminishing the cardiotoxicity associated with DOX therapy.

3.13. Hematological study

Marked decrease in blood cells count such as WBC count, RBC count, Hb content, platelet count were recorded after administration of free drug solutions for 7 days (Table 3). This might be possibly due to the direct contact of free drug with blood cells. The same amount of drug when encapsulated in various nanoparticulate (both plain and ligand conjugated) formulations reduced hematological toxicity. Further, in case of mice receiving CBSA-SLN-DOX formulation at a dose level of 5 mg/kg, almost no change in blood cells count was observed as compared to control group. This might possibly be due to the fact that, ligand anchored nanoparticulate formulations released their content i.e. drug directly to the target sites and very less amount of drug was leached out in blood during circulation. The results were in accordance with the results obtained previously by Jain et al. (2010) and Bhadra et al. (2005).

3.14. Evaluation of nephrotoxic and hepatotoxic effect

Serum urea/creatinine level and SGPT/AST/ALP level are used as markers of renal function and liver function, respectively. The serum urea and creatinine level ($p < 0.001$) were significantly increased upon administration of plain DOX (Table 4). However their elevation in the serum was least in animals administered with CBSA-SLN-DOX (5 mg/kg of DOX) (Table 4), indicating the formulation to evade damage to renal functions. This may be attributed to minimal quantity of CBSA conjugated SLNs encapsulating DOX gained access in kidney as compared to plain DOX.

In vivo hepatotoxicity induced by the anticancer drugs given in free/entrapped form was estimated in terms of serum glutamic pyruvic transaminase (SGPT), and alkaline phosphatase (ALP) and total bilurubin concentration. Free DOX induced toxicity in infected animals was reflected by the increased activity of SGPT (35.2 ± 3.2 IU/L), ALP (69.9 ± 4.7 IU/L) and AST concentration (29.7 ± 2.2 IU/L), while the encapsulated DOX in plain nanoparticles showed a small increase in the activity of SGPT (25.7 ± 1.7 IU/L), ALP (61.4 ± 4.6 IU/L) and AST (19.3 ± 2.1 IU/L). CBSA-SLN-DOX nanoparticles exhibited only a slight change in activity of these enzymes as compared with control animals (SGPT 16.5 ± 1.6 IU/L; ALP 54.8 ± 4.1 IU/L and AST 14.0 ± 1.5 IU/L) (Table 4). The differences

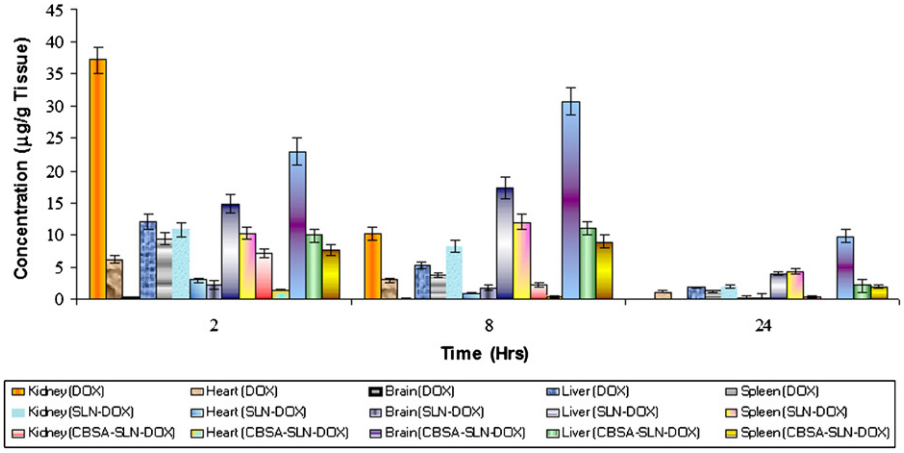

Fig. 15. Biodistribution of DOX obtained from plain DOX, SLN-DOX and CBSA-SLN-DOX in different tissues. Mean ± SD ($n = 6$; $p \leq 0.05$ (significant difference between plain DOX vs. SLN-DOX and CBSA-SLN-DOX; significant difference between SLN-DOX and CBSA-SLN-DOX)).

Table 4
Effect on kidney and liver function parameters in mice treated with plain DOX and formulations.

Code	Urea (mmol/L)	Creatinine (mmol/L)	SGPT (units/L)	ALP (units/L)	AST (units/L)
Control	7.1 ± 0.4	42.3 ± 1.9	14.5 ± 1.4	53.7 ± 4.2	13.2 ± 1.5
Plain DOX[*]	12.1 ± 0.6	75.6 ± 3.1	35.2 ± 3.2	69.9 ± 4.7	29.7 ± 2.2
SLN-DOX[*,a]	9.5 ± 0.6	60.2 ± 2.9	25.7 ± 1.7	61.4 ± 4.6	19.3 ± 2.1
CBSA-SLN-DOX[*,a]	7.4 ± 0.5	43.7 ± 2.0	16.5 ± 1.6	54.8 ± 4.1	14.0 ± 1.5

$n = 6$; $p \leq 0.05$.
[a] Significant difference between SLN-DOX and CBSA-SLN-DOX.
[*] Significant difference between free DOX vs. SLN-DOX and CBSA-SLN-DOX.

in the levels induced by free and nanoparticulate drugs after therapy were significant ($P \leq 0.05$). Serum analysis for SGPT, ALP, and AST illustrates that there was no evidence of biochemical toxicity in animals treated with CBSA conjugated SLNs.

Previously it had been reported that DOX itself at a dose of 2 mg/kg per 3 days caused a significant loss of body weight in mice as compared to nanoparticulate formulations (Park et al., 2006). From this study it may be concluded that CBSA anchored SLN formulations are safe for intravenous delivery of DOX so far as its toxicity is concerned. Similar results have been reported by Park et al. (2006) from *in vivo* subacute toxicity study of DOX loaded nanoparticles prepared using heparin–deoxycholic acid chemical conjugate. It means that CBSA-SLN-DOX as nanoparticulate formulations do not cause unexpected side effects and may be used as a safe drug carrier for drug delivery.

4. Conclusion

The article is first of this kind that provides an insight to use of CBSA coupled nanoconstructs for brain tumors exploiting adsorption mediated transcytosis to bypass the BBB. The present study reveals CBSA conjugated SLNs as efficient vectors for controlled sustained and targeted delivery. The formulation efficiently traversed large doses of anti-cancer drug across the BBB. This facilitates site-specific delivery, optimal therapeutic response and reduction in untoward side effects. However rigorous studies need to be performed to achieve any unambiguous generalization. The similar stratagem is also currently being investigated for spatial delivery of other chemotherapeutic agents to the brain.

Acknowledgement

The authors also thank Sun Pharma, Vadodara for providing doxorubicin HCl as gift sample and Bose Institute, Kolkata for FACS facility.

Appendix A. Supplementary data

Supplementary data associated with this article can be found, in the online version, at doi:10.1016/j.ijpharm.2011.09.039.

References

Agarwal, A., Asthana, A., Gupta, U., Jain, N.K., 2008. Tumour and dendrimers: a review on drug delivery aspects. J. Pharm. Pharmacol. 60, 671–688.
Agarwal, A., Gupta, U., Asthana, A., Jain, N.K., 2009a. Dextran conjugated dendritic nanoconstructs as potential vectors for anti-cancer agent. Biomaterials 30, 3588–3596.
Agarwal, A., Lariya, N., Saraogi, G.K., Dubey, N., Agrawal, H., Agrawal, G.P., 2009b. Nanoparticles as novel carrier for brain delivery: a review. Curr. Pharm. Des. 15, 917–925.
Ajith, T.A., Aswathy, M.S., Hema, U., 2008. Protective effect of *Zingiber officinale* Roscoe against anticancer drug doxorubicin-induced acute nephrotoxicity. Food Chem. Toxicol. 46, 3178–3181.
Begley, D., Sharma, H.S., Westman, J. (Eds.), 2003. Blood, Spinal Cord and Brain Barriers in Health and Disease. Elsevier Sci., USA, pp. 83–97.
Begley, D.J., Brightman, M.W., 2003. Structural and functional aspects of the blood–brain barrier. Prog. Drug Res. 61, 39–78.
Bhadra, D., Yadav, A.K., Bhadra, S., Jain, N.K., 2005. Glycodendrimeric nanoparticulate carriers of primaquine phosphate for liver targeting. Int. J. Pharm. 295, 221–233.
Bickel, U., Yoshikawa, T., Pardridge, W.M., 2001. Delivery of peptides and proteins through the blood–brain barrier. Adv. Drug Deliv. Rev. 46, 247–279.
Brigger, I., Morizet, J., Laudani, L., Aubert, G., Appel, M., Velasco, V., et al., 2004. Negative preclinical results with stealth nanospheres-encapsulated doxorubicin in an orthopic murine brain tumor model. J. Control. Release 100, 29–40.
Cavalli, R., Caputo, O., Carlotti, M.E., Trotta, M., Scarnecchia, C., Gasco, M.R., 1997. Sterilization and freeze-drying of drug-free and drug-loaded solid lipid nanoparticles. Int. J. Pharm. 148, 47–54.
Feng, Y., Zhou, Y., Zou, Q., Wang, J., Chen, F., Gao, Z., 2009. Preparation and characterization of bisphenol A-cationized bovine serum albumin. J. Immunol. Methods 340, 138–143.
Gulyaev, A.E., Gelperina, S.E., Skidan, I.N., Antropov, A.S., Kivman, G.Y., Kreuter, J., 1999. Significant transport of doxorubicin into the brain with polysorbate 80-coated nanoparticles. Pharm. Res. 16, 1564–1569.
Huang, M., Ma, Z., Khor, E., Lim, L.Y., 2002. Uptake of FITC-chitosan nanoparticles by A549 cells. Pharm. Res. 19, 1488–1494.
Injac, R., Perse, M., Obermajer, N., Djordjevic-Milic, V., Prijatelj, M., Djordjevic, A., Cerar, A., Strukelj, B., 2008. Potential hepatoprotective effects of fullerenol $C_{60}(OH)_{24}$ in doxorubicin-induced hepatotoxicity in rats with mammary carcinomas. Biomaterials 29, 3451–3460.
Jain, A., Agarwal, A., Majumder, S., Lariya, N., Khaya, A., Agrawal, H., et al., 2010. Mannosylated solid lipid nanoparticles as vectors for site-specific delivery of an anticancer drug. J. Control. Release 3, 359–367.
Juillerat-Jeanneret, L., 2008. The targeted delivery of cancer drugs across the blood–brain barrier: chemical modifications of drugs or drug-nanoparticles. Drug Discov. Today 13, 1099–1106.
Kolhe, P., Misra, E., Kannan, R.M., Kannan, S., Lieh- Lai, M., 2003. Drug complexation, *in vitro* release and cellular entry of dendrimers and hyperbranched polymers. Int. J. Pharm. 259, 143–160.
Lu, W., Sun, Q., Wan, J., She, Z., Jiang, X.G., 2006. Cationic albumin conjugated pegylated nanoparticles allow gene delivery into brain tumors via intravenous administration. Cancer Res. 66, 11878–11887.
Lu, W., Tan, Y.Z., Hu, K.L., Jiang, X.G., 2005. Cationic albumin conjugated pegylated nanoparticle with its transcytosis ability and little toxicity against blood–brain barrier. Int. J. Pharm. 295, 247–260.
Magenheim, B., Levy, M.Y., Benita, S., 1993. A new *in vitro* technique for evaluation of drug release profile from colloidal carriers-ultrafiltration technique at low pressure. Int. J. Pharm. 94, 115–123.
Martindale, 1996. The Extra Pharmacopoeia, 31st ed. Royal Pharmaceutical Society London, Pharmaceutical Press, London, p. 567.
Moghimi, S.M., Hunter, A.C., Murray, J.C., 2005. Nanomedicine: current status and future prospects. FASEB J. 19, 311–330.
Muller, R.H., Ruhl, D., Runge, S., Schulze-Foster, K., Mehnert, W., 1997. Cytotoxicity of solid lipid nanoparticles as a function of the lipid matrix and the surfactant. Pharm. Res. 4, 458–462.
Pardridge, W.M., 2003. Blood–brain barrier drug targeting: the future of brain drug development. Mol. Interv. 3, 90–105.
Park, K., Lee, G.Y., Kim, Y.S., Yu, M., Park, R.W., Kim, I.S., et al., 2006. Heparin–deoxycholic acid chemical conjugate as an anticancer drug carrier and its antitumor activity. J. Control. Release 114, 300–306.
Persidsky, Y., Ramirez, S.H., Haorah, J., Kanmogne, G.D., 2006. Blood–brain barrier: structural components and function under physiologic and pathologic conditions. J. Neuroimmunol. Pharm. 1, 223–236.
Petri, B., Bootz, A., Khalansky, A., Hekmatara, T., Muller, R., Uhl, R., et al., 2007. Chemotherapy of brain tumour using doxorubicin bound to surfactant-coated poly(butyl cyanoacrylate) nanoparticles: revisiting the role of surfactants. J. Control. Release 117, 51–58.
Reddy, L.H., Sharma, R.K., Chuttani, K., Mishra, A.K., Murthy, R.R., 2004. Etoposide-incorporated tripalmitin nanoparticles with different surface charge: formulation, characterization, radiolabeling and biodistribution studies. AAPS J. 6, 1–10.
Schinkel, A.H., 1999. P-glycoprotein, a gatekeeper in the blood–brain barrier. Adv. Drug Deliv. Rev. 36, 179–194.
Schubert, M.A., Muller-Goymann, C.C., 2003. Solvent injection as a new approach for manufacturing lipid nanoparticles—evaluation of the method and process parameters. Eur. J. Pharm. Biopharm. 55, 125–131.
Schwarz, C., Mehnert, W., 1999. Solid lipid nanoparticles (SLN) for controlled drug delivery. II. Drug incorporation and physicochemical characterization. J. Microencapsul. 16, 205–213.

Soni, V., Kohli, D.V., Jain, S.K., 2006. Transferrin coupled liposomes for enhanced brain delivery of doxorubicin. Vasc. Dis. Prev. 3, 31–38.
Storm, P.B., Moriarity, J.L., Tyler, B., Burger, P.C., Brem, H., Weingart, J., 2002. Polymer delivery of camptothecin against 9L gliosarcoma: release, distribution, and efficacy. J. Neurooncol. 56, 209–217.
Thole, M., Nobmanna, S., Huwyler, J., Bartmann, A., Fricker, G., 2002. Uptake of cationized albumin coupled liposomes by cultured porcine brain microvessel endothelial cells and intact brain capillaries. J. Drug Target. 103, 37–44.
Torchilin, V.P., 2005. Recent advances with liposomes as pharmaceutical carriers. Nat. Rev. Drug Discov. 41, 45–60.
Utreja, S., Jain, N.K., 2001. Solid lipid nanoparticles. In: Jain, N.K. (Ed.), Advances in Controlled and Novel Drug Delivery. CBS Publishers, New Delhi, pp. 408–425.
Vyas, S.P., Khar, R.K., 2002. Targeted and Controlled Drug Delivery Novel Carrier Systems, 1st ed. CBS Publishers, New Delhi, pp. 331–86.
Wiechelman, K.J., Braun, R.D., Fitzpatrick, J.D., 1988. BCA assay protocol. Anal. Biochem., 175.
Wong, H.L., Bendayan, R., Rauth, A.M., Xue, H.Y., Babakhanian, K., Wu, X.Y., 2006. A mechanistic study of enhanced doxorubicin uptake and retention in multidrug resistant breast cancer cells using a polymer–lipid hybrid nanoparticle system. J. Pharmacol. Exp. Ther. 317, 1372–1381.
Wu, D., Pardridge, W.M., 1999. Blood–brain barrier transport of reduced folic acid. Pharm. Res. 16, 415–419.
Xie, Y.L., Lu, W., Jiang, X.G., 2006. Improvement of cationic albumin conjugated pegylated nanoparticles holding NC-1900, a vasopressin fragment analog, in memory deficits induced by scopolamine in mice. Behav. Brain. Res. 173, 76–84.
Yadav, A.K., Mishra, P., Mishra, A.K., Mishra, P., Jain, S., Agrawal, G.P., 2007. Development and characterization of hyaluronic acid-anchored PLGA nanoparticulate carriers of doxorubicin. Nanomed. Nanotechnol. Biol. Med. 3, 246–257.
Yadav, A.K., Agarwal, A., Jain, S., Mishra, A.K., Bid, H., Rai, G., et al., 2010. Chondroitin sulphate decorated nanoparticulate carriers of 5-fluorouracil: development and *in vitro* characterization. J. Biomed. Nanotechnol. 6, 1–11.